Electronic Supplementary Material (ESI) for Dalton Transactions.
This journal is © The Royal Society of Chemistry 2023

Supporting Information

The {Cu_2I_2} module bearing metal organic frameworks: Crystal structures and fluorescence detecting performances to cysteine and explosive molecules

Jiang Jiang,*[,a] Zi-Wei Li,[b] Zhi-Zhuan Zhang,[b] Bin Tan[c], Zhao-Feng Wu*[,b] and Xiao-Ying Huang[b]

[a.] College of Life Sciences, Fujian Agriculture and Forestry University, Fuzhou, Fujian, 350002, P. R. China

[b.] State Key Laboratory of Structure Chemistry, Fujian Institute of Research on the Structure of Matter, Chinese Academy of Sciences, Fuzhou 350002, China.University of Chinese Academy of Sciences, Bejing, 100049, P. R. China.

[c.] School of Chemistry and Chemical Engineering, Beijing Institute of Technology, Beijing, 102488, P. R. China.

E-mail: jiang@fafu.edu.cn; zfwu@fjirsm.ac.cn

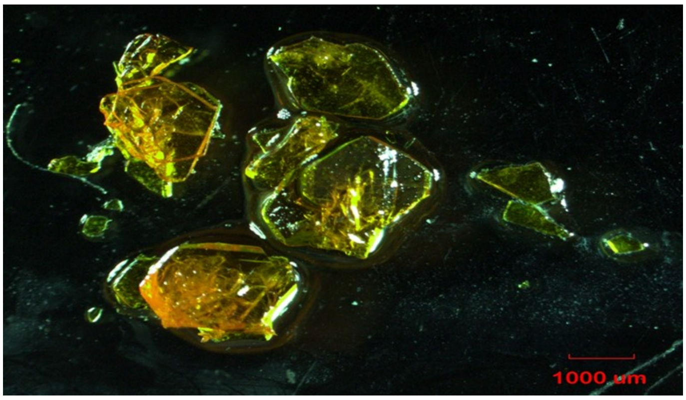

Figure S1. The photograph for the as-made Eu-CuI-INA crystals.

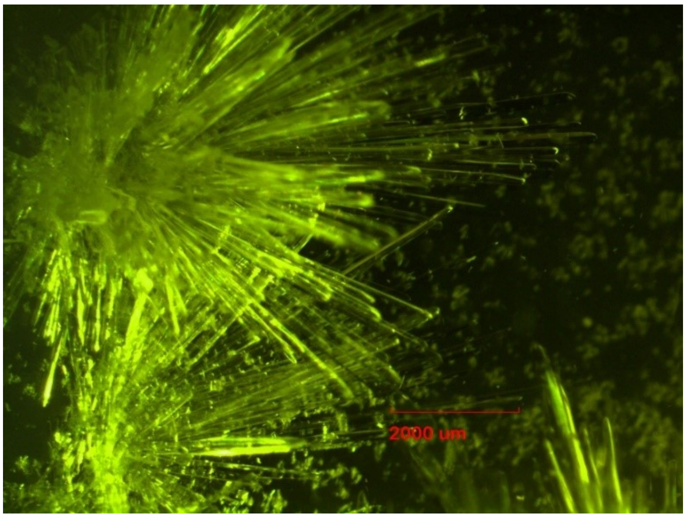

Figure S2. The photograph for the as-made Sr-K-CuI-INA crystals.

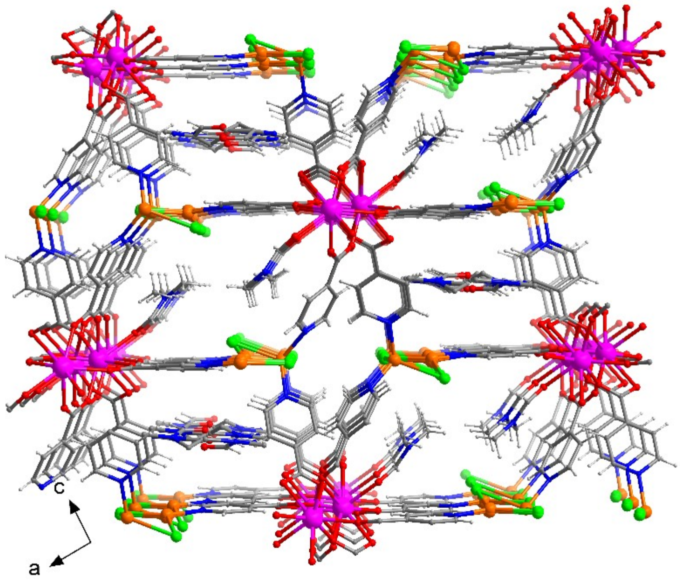

Figure S3. The 3D structure of Eu-CuI-INA viewed along the *b* axis, with the 1D channels occupied with DMF molecules.

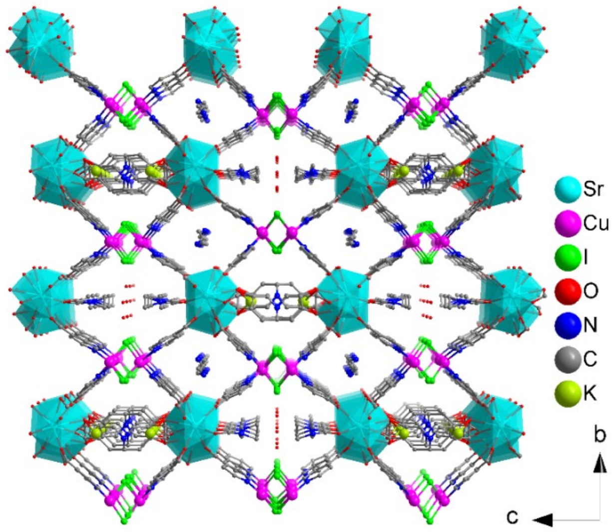

Figure S4. The 3D structure of Sr-K-CuI-INA viewed along the *a* axis. Hydrogen atoms are omitted for clarity.

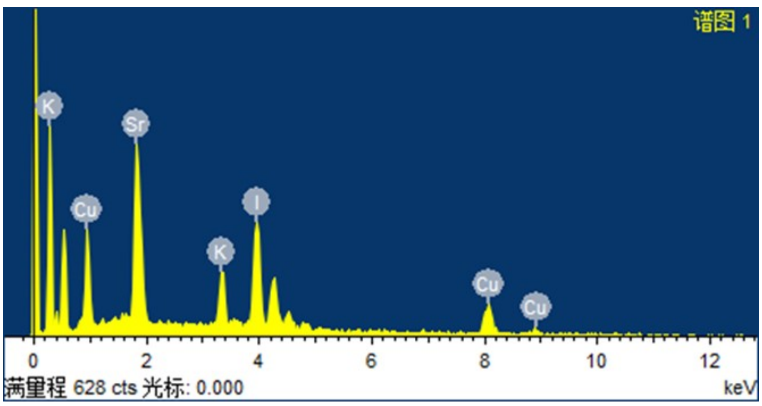

Figure S5. The EDS figure for the as-made Sr-K-CuI-INA sample.

Table S1. Selected bond lengths [Å] and angles [°] for compound Eu-CuI-INA.

Eu(1)-O(6)#1	2.4714(16)	I(2)-Cu(2)	2.635(7)
Eu(1)-O(3)	2.4851(17)	I(2)-Cu(2')	2.671(7)
Eu(1)-O(4)#2	2.5176(16)	I(2)-Cu(1)	2.807(6)
Eu(1)-O(5)#3	2.5214(15)	I(2')-Cu(2)	2.657(5)
Eu(1)-O(7)	2.5438(17)	I(2')-Cu(2')	2.698(4)
Eu(1)-O(1)#4	2.5989(16)	I(2')-Cu(1)	2.831(3)
Eu(1)-O(2)#5	2.6289(16)	Cu(1)-N(1)	2.1514(19)
Eu(1)-O(1)#5	2.7981(16)	Cu(1)-N(3)	2.1663(19)
I(1)-Cu(2')	2.746(2)	Cu(2)-N(2)	2.118(4)
I(1)-Cu(2)	2.760(4)	Cu(2')-N(2)	2.112(3)
I(1)-Cu(1)	2.8526(3)		
O(6)#1-Eu(1)-O(3)	74.83(6)	O(7)-Eu(1)-O(1)#4	74.75(6)
O(6)#1-Eu(1)-O(4)#2	76.97(6)	O(6)#1-Eu(1)-O(2)#5	73.67(6)
O(3)-Eu(1)-O(4)#2	122.01(6)	O(3)-Eu(1)-O(2)#5	136.99(6)
O(6)#1-Eu(1)-O(5)#3	121.39(6)	O(4)#2-Eu(1)-O(2)#5	77.76(6)
O(3)-Eu(1)-O(5)#3	78.78(6)	O(5)#3-Eu(1)-O(2)#5	143.47(5)
O(4)#2-Eu(1)-O(5)#3	74.52(6)	O(7)-Eu(1)-O(2)#5	77.07(6)
O(6)#1-Eu(1)-O(7)	143.58(6)	O(1)#4-Eu(1)-O(2)#5	103.61(5)
O(3)-Eu(1)-O(7)	141.06(6)	O(6)#1-Eu(1)-O(1)#5	79.21(5)
O(4)#2-Eu(1)-O(7)	76.03(6)	O(3)-Eu(1)-O(1)#5	94.74(5)
O(5)#3-Eu(1)-O(7)	73.52(6)	O(4)#2-Eu(1)-O(1)#5	127.81(5)
O(6)#1-Eu(1)-O(1)#4	133.09(6)	O(5)#3-Eu(1)-O(1)#5	154.80(5)
O(3)-Eu(1)-O(1)#4	78.05(6)	O(7)-Eu(1)-O(1)#5	98.78(5)
O(4)#2-Eu(1)-O(1)#4	149.56(5)	O(1)#4-Eu(1)-O(1)#5	65.67(6)
O(5)#3-Eu(1)-O(1)#4	89.13(5)	O(2)#5-Eu(1)-O(1)#5	51.07(5)
Eu(1)#7-O(1)-Eu(1)#6	114.34(6)		

Symmetry transformations used to generate equivalent atoms:

#1 -*x*+2,-*y*+1,-*z*+1; #2 -*x*+1,-*y*,-*z*+1; #3 *x*-1,*y*-1,*z*; #4 -*x*+3/2,*y*-1/2,-*z*+3/2; #5 *x*-1/2,-*y*+3/2,*z*-1/2; #6 *x*+1/2,-*y*+3/2,*z*+1/2 ; #7 -*x*+3/2,y+1/2,-*z*+3/2; #8 *x*+1,*y*+1,*z*.

Table S2. Selected bond lengths [Å] and angles [°] for compound Sr-K-CuI-INA.

Sr(1)-O(3)#1	2.485(5)	Sr(1)-O(4B)	2.806(11)
Sr(1)-O(4)	2.509(8)	Cu(1)-N(2)#3	2.047(6)
Sr(1)-O(2)#2	2.527(5)	Cu(1)-N(1)	2.052(5)
Sr(1)-O(6)	2.553(4)	Cu(1)-I(2)#4	2.570(3)
Sr(1)-O(1)	2.600(6)	Cu(1)-I(1)	2.6440(11)
Sr(1)-O(3)	2.639(5)	Cu(1)-I(2)	2.713(4)
Sr(1)-O(7)	2.664(5)	O(5)-K(1)#5	2.735(12)
Sr(1)-O(2)	2.700(5)	O(3)-K(1)#5	3.333(8)
Sr(1)-O(5)	2.781(11)		
O(3)#1-Sr(1)-O(4)	103.9(2)	O(4)-Sr(1)-O(7)	114.85(19)
O(3)#1-Sr(1)-O(2)#2	79.47(17)	O(2)#2-Sr(1)-O(7)	87.08(12)
O(4)-Sr(1)-O(2)#2	157.9(2)	O(6)-Sr(1)-O(7)	155.40(4)
O(3)#1-Sr(1)-O(6)	90.13(14)	O(1)-Sr(1)-O(7)	78.81(19)
O(4)-Sr(1)-O(6)	85.9(2)	O(3)-Sr(1)-O(7)	70.36(15)
O(2)#2-Sr(1)-O(6)	72.24(14)	O(3)#1-Sr(1)-O(2)	146.43(16)
O(3)#1-Sr(1)-O(1)	151.4(2)	O(4)-Sr(1)-O(2)	101.0(2)
O(4)-Sr(1)-O(1)	90.1(3)	O(2)#2-Sr(1)-O(2)	69.19(19)
O(2)#2-Sr(1)-O(1)	96.9(2)	O(6)-Sr(1)-O(2)	69.45(13)
O(6)-Sr(1)-O(1)	116.03(16)	O(1)-Sr(1)-O(2)	48.87(16)
O(3)#1-Sr(1)-O(3)	69.3(2)	O(3)-Sr(1)-O(2)	144.00(16)
O(4)-Sr(1)-O(3)	50.3(2)	O(7)-Sr(1)-O(2)	116.06(15)
O(2)#2-Sr(1)-O(3)	145.53(15)	O(3)#1-Sr(1)-O(5)	83.6(3)
O(6)-Sr(1)-O(3)	120.55(17)	O(4)-Sr(1)-O(5)	44.7(3)
O(1)-Sr(1)-O(3)	103.5(2)	O(2)#2-Sr(1)-O(5)	115.6(2)
O(3)#1-Sr(1)-O(7)	72.69(17)	O(6)-Sr(1)-O(5)	46.0(2)
O(1)-Sr(1)-O(5)	122.5(3)	O(7)-Sr(1)-O(5)	143.7(2)
O(3)-Sr(1)-O(5)	75.8(2)	O(3)#1-Sr(1)-O(4B)	113.9(2)
O(2)-Sr(1)-O(5)	98.9(3)	O(2)#2-Sr(1)-O(4B)	166.6(2)

O(6)-Sr(1)-O(4B)	107.3(3)	O(3)-Sr(1)-O(4B)	46.6(2)
O(1)-Sr(1)-O(4B)	71.0(3)	O(7)-Sr(1)-O(4B)	95.9(3)
O(2)-Sr(1)-O(4B)	97.9(2)	O(5)-Sr(1)-O(4B)	68.8(3)
N(2)#3-Cu(1)-N(1)	107.9(2)	I(2)#4-Cu(1)-I(2)	5.4(3)
I(1)-Cu(1)-I(2)	117.45(13)	O(5)#10-K(1)-O(3)#10	65.7(2)
O(5)#5-K(1)-O(3)#10	70.1(3)		

Symmetry transformations used to generate equivalent atoms:

#1 -*x*+2,-*y*,*z*; #2 -*x*+1,-*y*,*z*; #3 *x*-3/2,-*y*+1/2,-*z*+1/2; #4 *x*,*y*,-*z*+1; #5 -*x*+1,-*y*,-*z*; #6 *x*,*y*,-*z*; 7 -*x*,-*y*,-*z*; #8 *x*+1/2,-*y*+1/2,-z+1/2; #9 *x*+3/2,-*y*+1/2,-*z*+1/2; #10 *x*-1,*y*,-*z*; #11 *x*-1/2,-*y*+1/2,-*z*+1/2

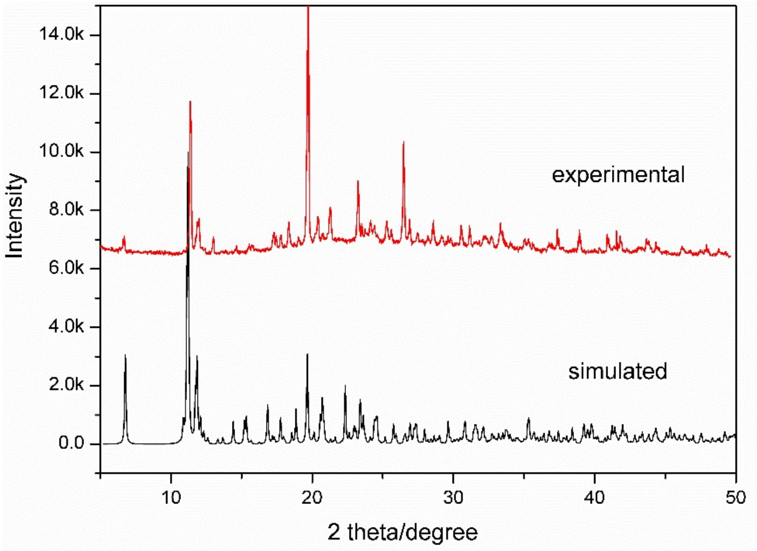

Figure S6. The PXRD patterns for the as-made Eu-CuI-INA.

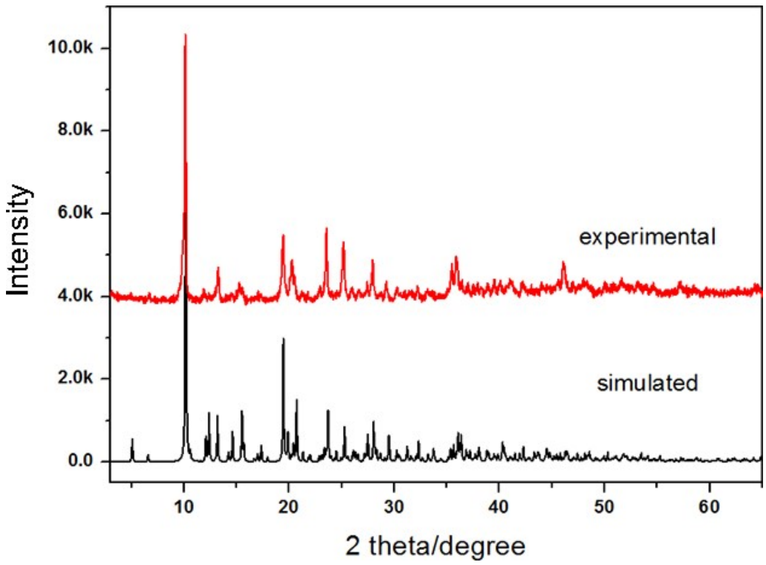

Figure S7. The PXRD patterns for the as-made Sr-K-CuI-INA.

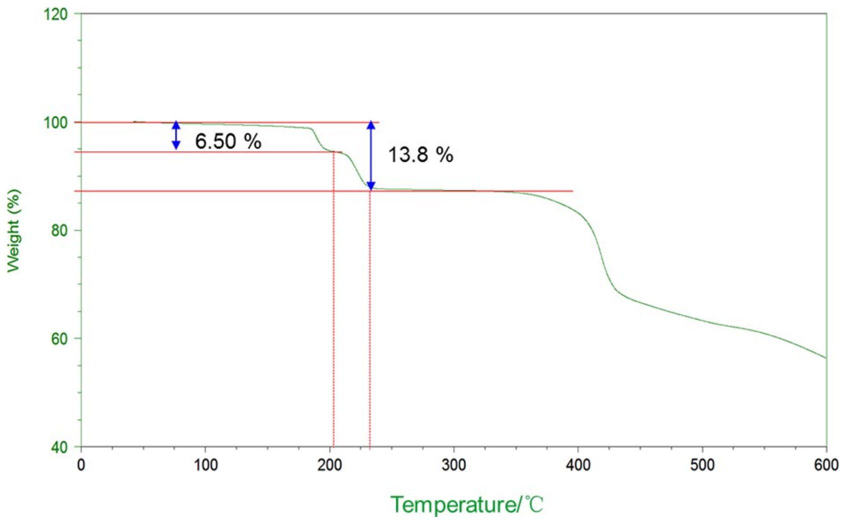

Figure S8. The TG curve for the as-made Eu-CuI-INA.

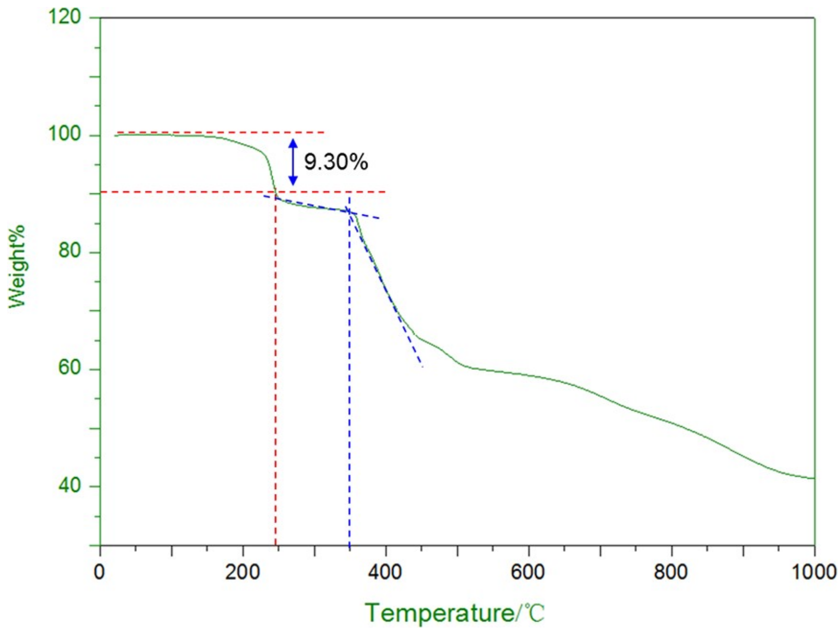

Figure S9. The TG curve for the as-made Sr-K-CuI-INA.

As depicted in Fig. S8, the first weight loss of 6.5% around 200 °C is ascribed to the loss of the free DMF (Calculated 6.83%), and then a second weight loss of 13.8% was observed around 230 °C, which could be ascribed to the loss of the coordinated DMF molecules (Calculated 14.01% for the removing of all DMF molecules). Then a platform ranging from 230 to 400 °C was observed after which the framework began to collapse. As shown in Fig. S9, the first weight loss of 9.30 % around 245 °C would be generated from the loss of the cationic $[NH_2(CH_3)_2]^+$, water and DMF molecules (Calculated 8.77%). Then a continuous slow weight loss appeared ranging from 245 to 350 °C after which a sharp stage of weight loss occurred which should correspond to the collapse of its structure.

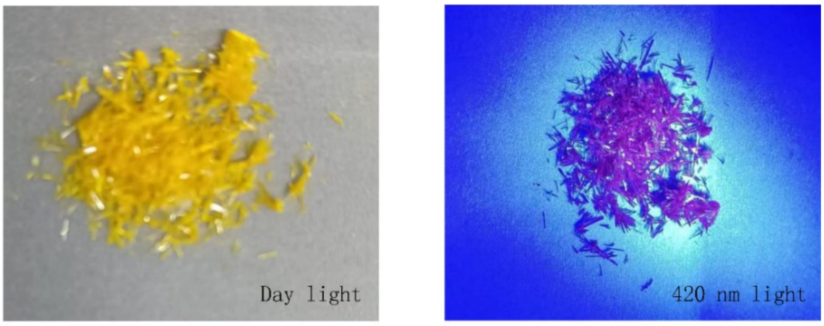

Figure S10. The photographs for the as-made Sr-K-CuI-INA under day light and 420 nm light.

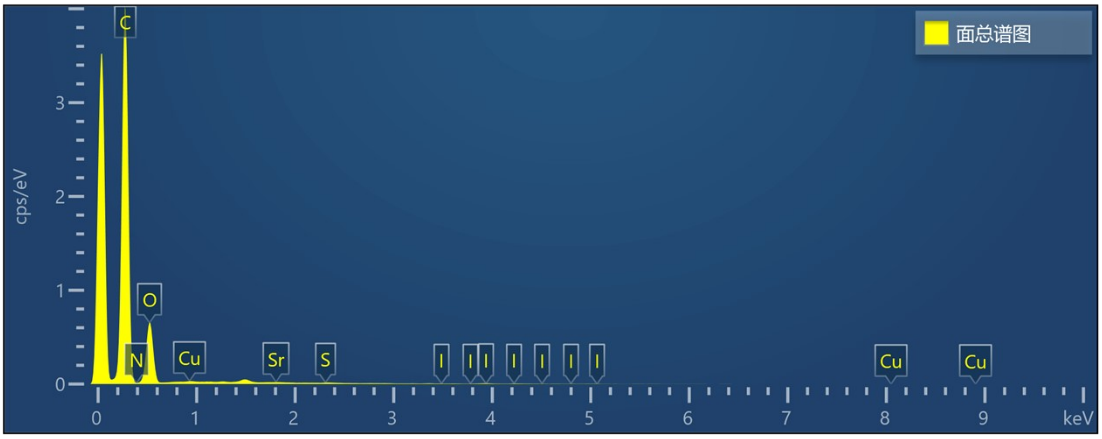

Figure S11. The EDS measurement for the Cys immersing sample.

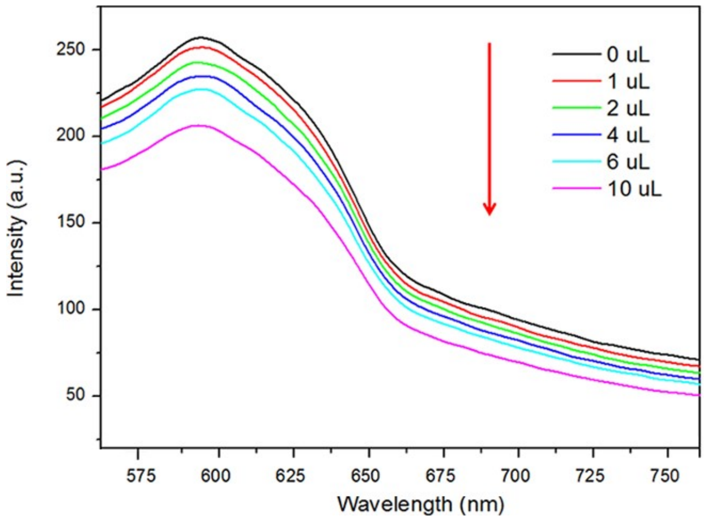

Figure S12. The fluorescence spectra of Sr-K-CuI-INA with the addition of nitrobenzene.

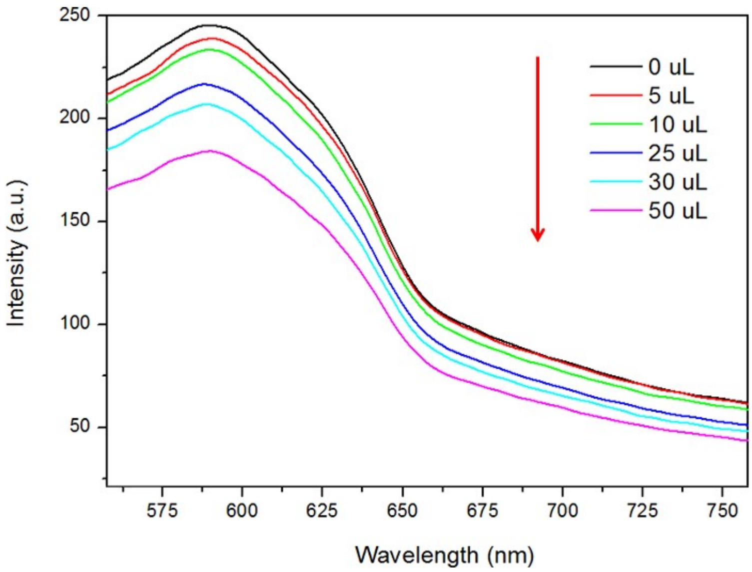

Figure S13. The fluorescence spectra of Sr-K-CuI-INA with the addition of 10^{-3} M 4-nitroaniline.

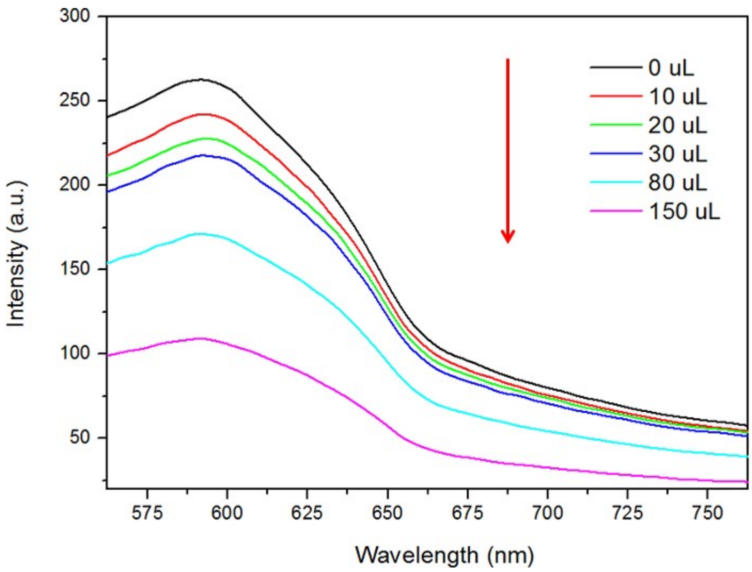

Figure S14. The fluorescence spectra of Sr-K-CuI-INA dispersed in the 10^{-3} M nitrobenzene with the addition of 10^{-3} M TNP.

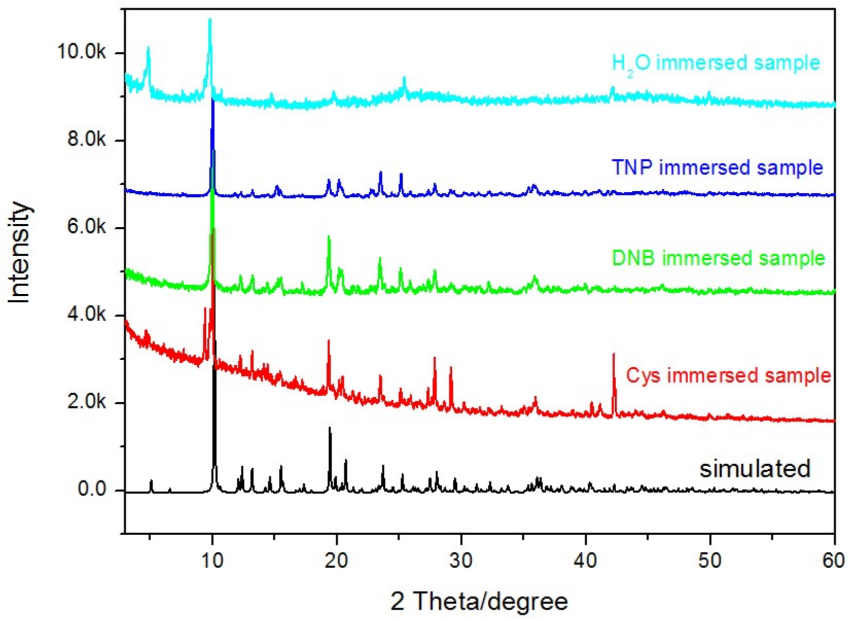

Figure S15. The PXRD patterns for the Sr-K-CuI-INA immersed in the 10^{-2} M Cys, 10^{-3} M DNB and TNP, and H_2O over 12 hours.

Table S3 The selected MOF sensors for FL detecting of TNP.

MOF sensors	K_{sv} / M^{-1}	**Reference**
$Ca_6(tatb)_4(H_2O)(DMF)_4$	6.8×10^4	
$Ca_6(tatb)_4(H_2O)(DMA)_4$	4.4×10^4	1
$Ca_6(tatb)_4(H_2O)(DEF)_4$	1.8×10^4	
$Cd(NDC)_{0.5}(PCA)$	3.5×10^4	2
$[(CH_3)_2NH_2]_3[Zn_4Na(BPTC)_3]\cdot 4CH_3OH\cdot 2DMF$	3.2×10^4	3
$Cd(NDC)(H_2O)$	2.385×10^4	4
$Zn(NDC)(H_2O)$	6.0×10^4	
$[Tb(L)_{1.5}(H_2O)]\cdot 3H_2O$	7.47×10^4	5
$Zr_6O_4(OH)_6(L)_6$	2.9×10^4	6
$[Eu_3(L)_3(HCOO)(\mu_3\text{-}OH)_2(H_2O)]\cdot$ solvents	2.1×10^4	7
$Zn_8(ad)_4(BPDC)_6O\cdot 2Me_2NH_2$	4.6×10^4	8
$Zr_6O_4(OH)_6(L)_6$	5.8×10^4	9
$[Cd(NDC)L]_2\cdot H_2O$	3.7×10^4	10
$[Zn(BINDI)_{0.5}(bpa)_{0.5}(H_2O)]\cdot 4H_2O$	4.9×10^4	11
$[Zn(BINDI)_{0.5}(bpe)]\cdot 3H_2O$	1.29×10^4	
Cu-CIP	1.07×10^4	12
$(Me_2NH_2)_4[Eu_4(DDAC)_3(HCO_2)(OH_2)_2]\cdot 8DMF\cdot 9H_2O$	8.6×10^4	13
$[Zn_3(TIAB)_2(IMDC)_2]\cdot(NO_3)_2\cdot(DMF)_2\cdot(H_2O)_2$	5.68×10^4	14
Zn(bipa)(suc)	6.48×10^4	15
$Zn_4(DMF)(Ur)_2(NDC)_4$	1.08×10^5	16
$\{Mn(Tipp)(A)_2\}_n\cdot 2H_2O$	1.18×10^5	17

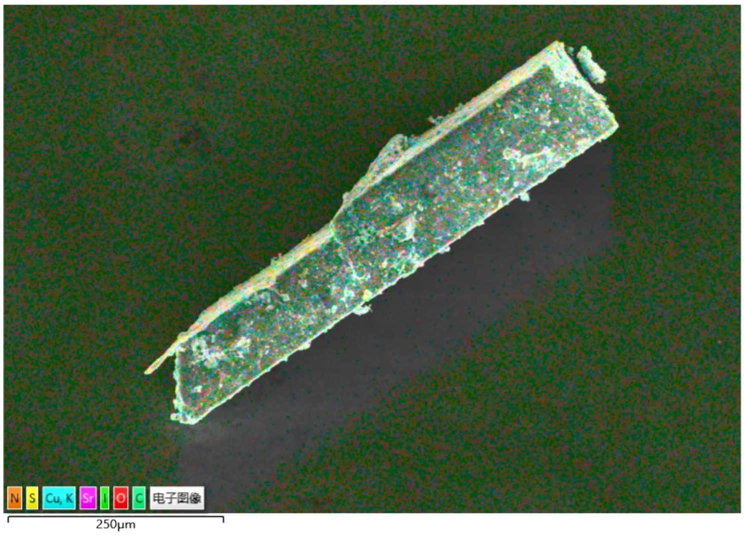

Figure S16. The SEM photograph with elements mapping for the Cys immersing sample.

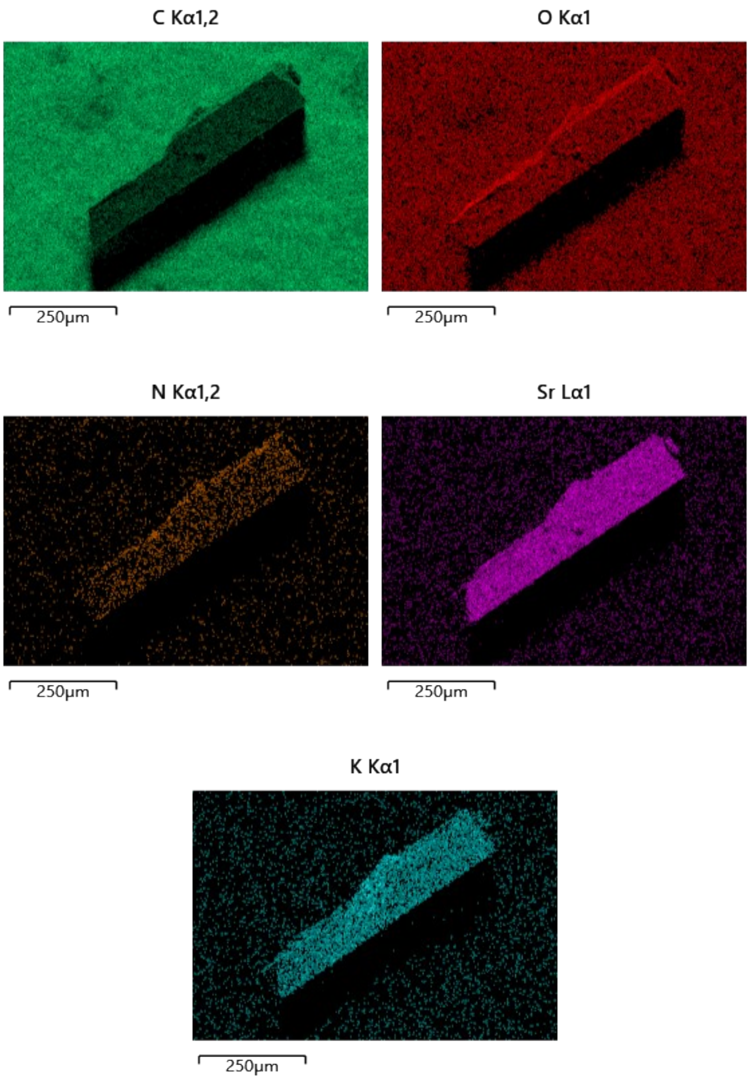

Figure S17. The C, N, O, Sr, K mapping for the Cys immersing sample.

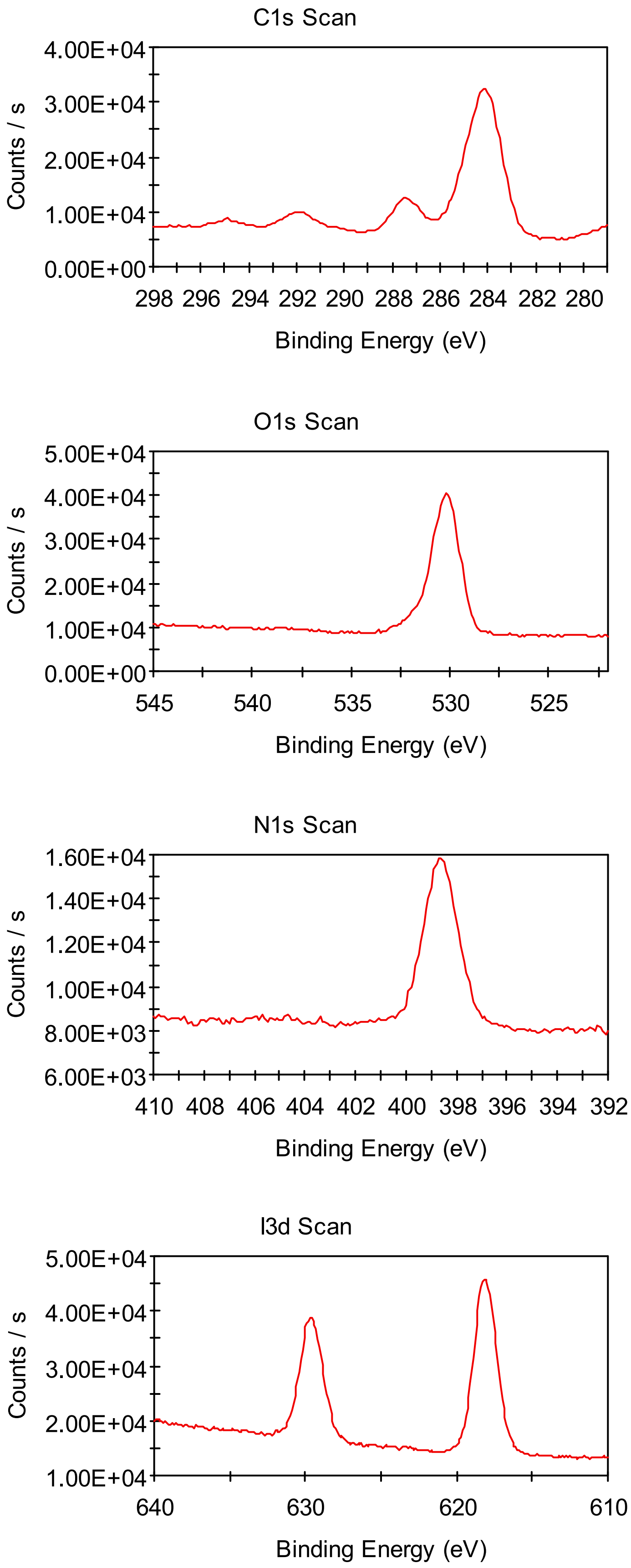

Figure S18. The X-ray photoelectron spectroscopy (XPS) spectra of C 1s, O1s, N 1s and I 3d for the Cys immersed sample.

References:

1. B. Tan, X.-Z. Hei, Y.-P. Lin, Z.-F. Wu and X.-Y. Huang, *J. Mater. Chem. C*, 2023, DOI: 10.1039/D3TC03053A.
2. S. S. Nagarkar, B. Joarder, A. K. Chaudhari, S. Mukherjee and S. K. Ghosh, *Angew. Chem. Int. Ed.*, 2013, **52**, 2881.
3. E.-L. Zhou, P. Huang, C. Qin, K.-Z. Shao and Z.-M. Su, *J. Mater. Chem. A*, 2015, **3**, 7224.
4. P. Ghosh, S. K. Saha, A. Roychowdhury and P. Banerjee, *Eur. J. Inorg. Chem.*, 2015, 2851.
5. L.-H. Cao, F. Shi, W.-M. Zhang, S.-Q. Zang and T. C. W. Mak, *Chem. Eur. J.*, 2015, **21**, 15705.
6. S. S. Nagarkar, A. V. Desai and S. K. Ghosh, *Chem. Commun.*, 2014, **50**, 8915.
7. X.-Z. Song, S.-Y. Song, S.-N. Zhao, Z.-M. Hao, M. Zhu, X. Meng, L.-L. Wu and H.-J. Zhang, *Adv. Funct. Mater.*, 2014, **24**, 4034.
8. B. Joarder, A. V. Desai, P. Samanta, S. Mukherjee and S. K. Ghosh, *Chem. Eur. J.*, 2015, **21**, 965.
9. S. S. Nagarkar, A. V. Desai, P. Samanta and S. K. Ghosh, *Dalton Trans.*, 2015, **44**, 15175.
10. B.-Q. Song, C. Qin, Y.-T. Zhang, X.-S. Wu, L. Yang, K.-Z. Shao and Z.-M. Su, *Dalton Trans.*, 2015, **44**, 18386
11. S. S. Dhankhar, N. Sharma and C. M. Nagaraja, *Inorg. Chem. Front.*, 2019, **6**, 1058.
12. M. Kaur, M. Yusuf and A. K. Malik, *J. Fluores.*, 2021, **31**, 1959.
13. H. Chen, Z. Zhang, T. Hu and X. Zhang, *Inorg. Chem. Front.*, 2021, **8**, 4376.
14. Y. Liu, Y. Wang, Y. Zhang, P. G. Karmaker, L. Zhang, F. Huo, X. Yang and B. Zhao, *Dyes and Pigments*, 2022, **199**, 110099.
15. S.-S. Ge, Y.-H. Zhang, X.-Q. Yang and X.-G. Mu, *Trans. Metal Chem.*, 2023, **48**, 37.
16. S. Mukherjee, A. V. Desai, B. Manna, A. I. Inamdar and S. K. Ghosh, *Cryst. Growth. Des.*, 2015, **15**, 4627.
17. Y. Zou, K. Huang, X. Zhang, D. Qin and B. Zhao, *Inorg. Chem.*, 2021, **60**, 11222.